Am J Transl Res 2015;7(1):162-174
www.ajtr.org /ISSN:1943-8141/AJTR0002864

Original Article

Notch signaling induces epithelial-mesenchymal transition to promote invasion and metastasis in adenoid cystic carcinoma

Zhi-Li Zhao[1*], Si-Rui Ma[1*], Wei-Ming Wang[1], Cong-Fa Huang[1], Guang-Tao Yu[1], Tian-Fu Wu[1], Lin-Lin Bu[1], Yu-Fan Wang[1], Yi-Fang Zhao[2], Wen-Feng Zhang[2], Zhi-Jun Sun[2]

[1]The State Key Laboratory Breeding Base of Basic Science of Stomatology & Key Laboratory of Oral Biomedicine Ministry of Education, [2]Department of Oral Maxillofacial-Head Neck Oncology, School and Hospital of Stomatology, Wuhan University, Wuhan, China. [*]Equal contributors and co-first authors.

Received September 28, 2014; Accepted October 30, 2014; Epub January 15, 2015; Published January 30, 2015

Abstract: Epithelial-mesenchymal transition (EMT) is considered to have pivotal roles in the invasive and metastatic of Adenoid cystic carcinoma (AdCC) which is marked by local infiltration and distant metastasis. Notch signaling abnormity has been implicated as important molecular events in recent next generation sequencing studies of AdCC, but the detail is still unclear. This study was designed to investigate the expression of Notch signaling pathway and its relation with EMT program in AdCC. We constructed custom-made Tissue microarray (TMA) to evaluate the immunoreactivity of Notch signaling and EMT program and found that Notch signaling increase consecutively from NSG, PMA to AdCC, suggesting Notch signaling pathway may be associated with human AdCC progression. Then, we carried out Pearson correlation analysis and showed a close correlation of Notch signaling and EMT progression. When blocking Notch signaling pathway with γ-secretase inhibitor DAPT, EMT progression was decreased and migration and invasion ability were declined. Collectively, these findings suggest the vital roles of Notch signaling pathway in AdCC progression through their relationship with EMT progress. Targeting Notch signaling may provide further understanding of the mechanism of invasion and metastasis of AdCC as well as potential clinical therapeutics.

Keywords: Head and neck cancer, adenoid cystic carcinoma, epithelial-mesenchymal transition, Notch signaling

Introduction

Adenoid cystic carcinoma (AdCC) is a relatively rare and morphologically diverse malignant tumor that arises from the secretory epithelial cells of major and minor salivary glands and accounts for approximately 10% of all salivary neoplasms [1]. Typically, Adenoid cystic carcinoma has been characterized by a protracted clinical course yet insidious invasion into adjacent tissue and hematogenous spread to distant organs [2]. However, up to now, the precise mechanisms underlying the invasion and metastasis are yet not clearly elucidated. Better understanding of the biological factor regulating AdCC invasion and metastasis may result in more effective treatment options and more accurate prognostic consultation in AdCC.

Among the multiple molecular mechanisms that are dysregulated in Adenoid cystic carcinoma, accumulating evidence shows the importance of the Notch signaling pathway. Notch signaling defines an evolutionary conservative pathway, which plays a fundamental role in the implementation of differentiation, proliferation, and apoptosis programs [3]. Many reports have suggested the implication of aberrant Notch signaling pathway in the tumor progression, including colon cancer, T-cell leukemia and head and neck cancer [4-7]. As regards for AdCC, whole-genome sequence analysis indicates a 13% NOTCH1 gene mutations, and exon sequencing in a series of 24 ACC samples also identifies this finding [7, 8]. These alterations indicate the possible therapeutic implications, but further characterization for the expression pattern and levels of Notch1 in AdCC remain unknown, and the exact mechanism remains to be further explored.

Recent evidences have demonstrated that Epithelial-mesenchymal transition (EMT) has a crucial role in the invasion and metastasis of

AdCC. EMT process depicts a set of rapid changes in the cellular phenotype in which epithelial cells experience a molecular switch from a polarized, epithelial phenotype to a highly motile, non-polarized mesenchymal phenotype, providing tumor cells with the ability to escape from the primary tumor, to migrate to distant regions, and to invade tissues [9, 10]. Transforming growth factor-beta 1 (TGF-β1) and Slug are two representative molecules involved in EMT regulation progress [11, 12]. Multiple studies have shown that TGF-β1 enhances the metastatic and invasive properties of various cancer types, suggesting that it induces epithelial-mesenchymal transition in cancer cells [13, 14]. We also have previously reported that Slug-mediated EMT-like transformation plays an important role in the process of metastasis and apoptosis of adenoid cystic carcinoma *in vitro* study [15]. However, the relation of Notch signaling with EMT is unclear and the specific mechanism is to be determined.

Based on the above considerations, in this study, we investigated the expression pattern and levels of Notch signaling using customer-made tissue microarray (TMA), also EMT program related proteins were assessed using TMA serial sections. Besides, correlation analysis and hierarchical cluster were used to evaluate the relation of Notch signaling and EMT program. Furthermore, we used γ-secretase inhibitor DAPT to block the Notch signaling, and found reduced EMT progression as expected. These data implicate the important roles of Notch signaling in AdCC progression through their combination with TGF-β1 and Slug-mediated EMT progress and potential therapeutic target.

Materials and methods

Ethics statement and patients' specimens

This study was performed with the approval of the Medical Ethics Committee of Hospital of Stomatology, Wuhan University (PI: Zhi-Jun Sun), and written medical informed consent was acquired from each patient before surgery. All the patients' specimens were diagnosed by two expert pathologists and came from the Department of Oral and Maxillofacial Surgery, School and Hospital of Stomatology, Wuhan University, which included 72 AdCC specimens, 12 pleomorphic adenoma samples and 25 normal salivary gland specimens. AdCC histological subtype was ranked according to the World Health Organization's classification of salivary gland tumor [16].

Tissue microarray construction

High-density tissue microarrays (TMAs) were constructed from the paraffin-embedded histopathological blocks in collaboration with the Shanghai Biochip Company, Ltd, Shanghai, China, as described previously [17]. To put it simply, Hematoxylin and eosin stained slides of the specimen blocks were firstly reviewed, then areas representative of the characteristic histological patterns in each case were selected for inclusion in the tissue microarrays, 1.5 mm diameter cores were punched for construction of tissue microarrays. Serial 3-μm sections from the TMAs were cut and prepared for subsequent immunohistochemical analysis.

Immunohistochemical staining and digital evaluation

Immunohistochemistry for tissue microarray was carried out as previously described [18]. Briefly, microarray sections were firstly deparaffinized and hydrated, then antigen retrieval was performed at pH 6.0 citrate buffer solutions. After cooling down to room temperature, sections were incubated with 3% hydrogen peroxide to quench endogenous peroxidase activity. The sections were incubated at 4°C overnight with respective primary antibodies and then washed with phosphate buffered saline (PBS), after that the sections were incubated with biotin-labeled secondary antibody for 30 minutes and then streptavidin peroxidase for 30 minutes. Finally, sections were adequately rinsed with 1X PBS, 3, 3-diaminobenzidine (DAB) de] velopment and Hematoxylin counterstaining, routine rehydration and mounting slides. For digital evaluation, tissue microarray sections were scanned and digitized with Aperio Scan] Scope Slide Scanner (Vista, CA, USA) system, and histoscores was quantified using Aperio ImageScope (version12.0) and calculated using the formula previously described [19].

Hierarchical clustering and data visualization

Firstly, histoscores the sections were converted to scaled values centered on zero, then the Pearson's correlation coefficient was carried out with Cluster 3.0 with average linkage to achieve the hierarchical analysis [20], and the

Table 1. Primers used real-time RT-PCR

Gene		Primers	Size (bp)
TGFβ1	F	TTAACATCTCCAACCCAGCG	121
	R	TCCTGTCTTTATGGTGAAGCC	
SLUG	F	CAAGGACACATTAGAACTCACAC	199
	R	CTACACAGCAGCCAGATTCC	
E-cadherin	F	ATCTGTTGCAGAAGGCGCTCTT	100
	R	TGTAGGCGATGGCAGCATTGT	
NOTCH1		CGGGTCCACCAGTTTGAATG	76
		GTTGTATTGGTTCGGCACCAT	
HES1	F	GGACAAACCAAAGACGGCCTCTGAGCACAG	141
	R	TGCCGGGAGCTATCTTTCTTAAGTGCATCC	
GAPDH	F	AGCCTCAAGATCATCAGCAATGCC	105
	R	TGTGGTCATGAGTCCTTCCACGAT	

results were visualized using the Java TreeView 1.1.6 version [21].

Cell lines, antibodies and reagent

Human salivary adenoid carcinoma cell lines SACC-83 (low metastasis and invasion rate) and SACC-LM (high metastasis and invasion rate) were gifted from School and Hospital of Stomatology, Peking University and implemented in this study. The following antibodies were used in this study: NICD (Notch intracellular domain, NICD), active isotype of Notch1), HES1, Slug (dilution 1:400, 1:200, 1:400 and 1:200 respectively) from Cell Signaling Technology, Inc., (Danvers, MA, USA), monoclonal rabbit anti-human TGF-β1 (1:200) from Epitomics, Inc. (Burlingame, CA, USA), polyclonal rabbit anti-human E-cadherin (1:200) from Proteintech Group, Inc. (Campbell, Chicago, USA). γ-secretase DAPT was purchased from Selleck Chemicals, (Houston, TX, USA), and prepared in dimethyl sulfoxide (DMSO) as 20 mM stock solution stored at -20°C and used at a final concentration of 10 μM.

Quantitative real-time RT-PCR

Quantitative Real-Time RT-PCR was performed to evaluate the expression of Notch signaling and EMT-related genes in AdCC cell lines. In brief, total cell RNA was extracted with Trizol (Takara, Kyoto, Japan) and treated with RNase-free DNase I (Takara) to avoid genomic DNA contamination, RNA aliquots (1 μg) was reversed to cDNA (20 μl) using PrimeScript™ RT Kit (Takara). Then, PCR amplification of the 2 μl cDNA template was carried out using SYBR® Premix EX Taq™IIqPCR mix (Takara) on ABI7500 Real-Time PCR system (Applied Biosystems). GAPDH or 18sRNA was used as an internal control, and reactions were run in triplicate, and the results were averaged. **Table 1** showed the primer sequences used in this study. The relative expression level of the genes was calculated using the ΔΔCt method.

Western blotting analysis

Total proteins were isolated from cultured SACC-83 or SACC-LM cells using M-PER Mammalian Protein Extraction Reagent (Pierce, Rockford, IL), and concentrations were detected by BCA assay kit (Pierce). Subsequently, 30 μg proteins from each sample were separated by 10% SDS-polyacrylamine gel and transferred electrophoretically to polyvinylidene difluoride (PVDF) membranes (Millipore, Bedford, MA). Membranes were blocked with 5% bovine serum albumin (BSA) in TBS containing 0.1% tween 20 (TBST) at room temperature for 60 minutes, then incubated overnight with primary antibody respectively at dilutions recommended by the manufactures. After fully incubation, bolts were detected by horseradish peroxidase–conjugated anti-mouse or anti-rabbit secondary antibody, and visualized with the SuperSignal West Femto maximum sensitivity substrate (Thermo Scientific, Rockford, IL, USA) on X-ray film. The images on X-ray films were then converted to electronic format using digital Scanner System (CanoScan LiDE110) and the density was calculated with ImageJ software packages.

Immunofluorescence analysis

SACC-83 or SACC-LM cells were seeded onto coverslips at a density of 10^5/mL and cultured in a 6-well plate for 24 hours with the indicated treatment. After treatment, cells were washed twice in PBS and fixed in 4% paraformaldehyde for 30 minutes. Then cells were permeabilized in 0.2% Triton X-100 in PBS for 15 minutes, and blocked by non-immune goat serum for 60 minutes at room temperature. Then cells were incubated at 4°C overnight respectively, with primary antibody at dilutions recommended by the manufactures, after the PBS washout, PerCP-Cy5.5-conjugated secondary antibody (1:200. Jackson ImmunoResearch, USA) was

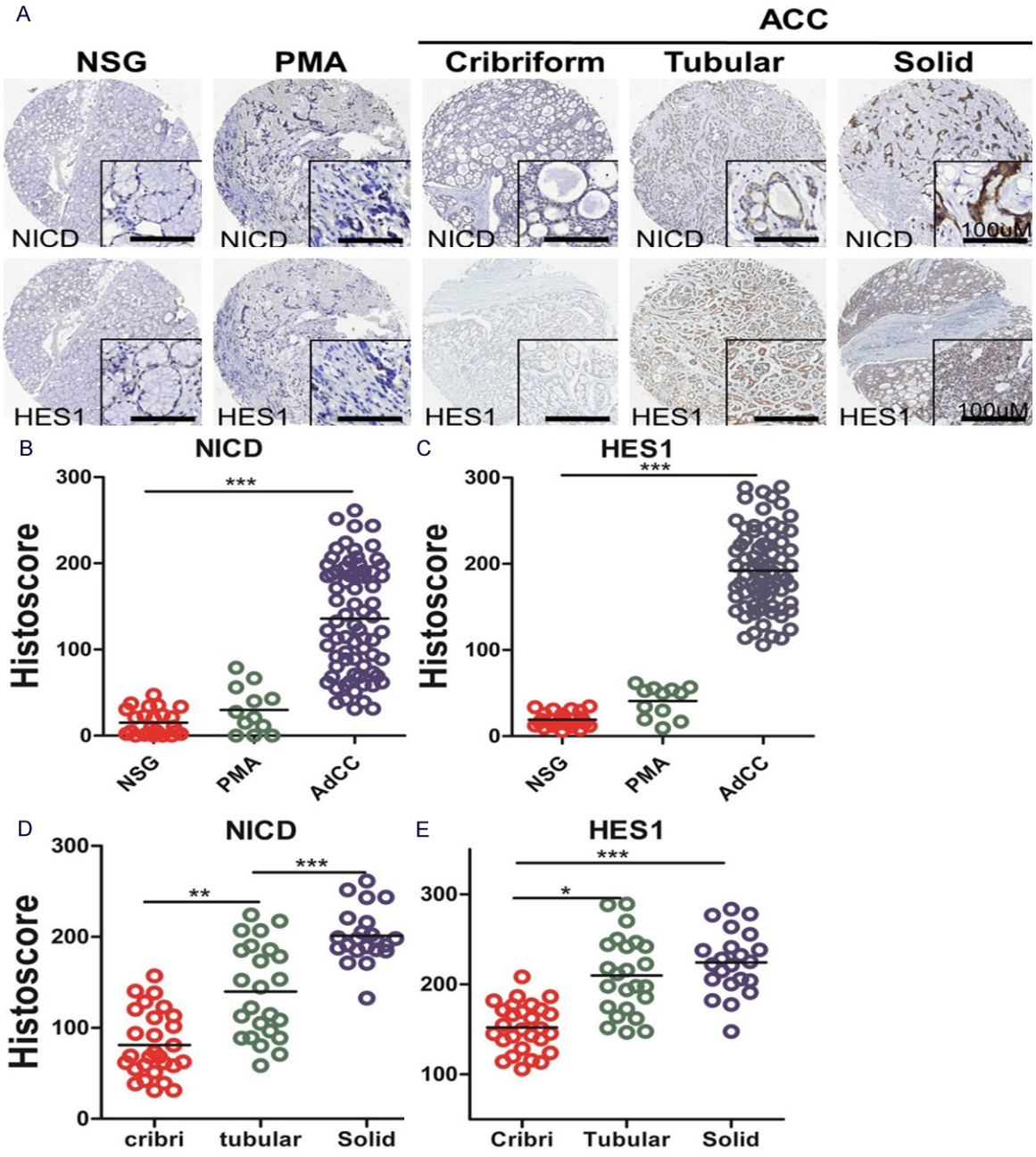

Figure 1. Notch was increased in AdCC and may be associated with human AdCC progression: A. Representative immunohistochemical staining of NICD and HES1 in human AdCC tissue (right panel) compared with normal salivary gland (NSG, left panel), pleomorphic adenoma (PMA, middle panel) (Scale bars = 100 μm); B and C. Quantitative assess of Histoscores of NICD and HES1 expression in NSG, PMA and AdCC, NICD and HES1 levels in AdCC was higher when compared with NSG an PMA (***P < 0.001; One-way ANOVA); D. Comparison between different pathology types of NICD and HES1, expression of NICD or HES1 was statistically different between cribriform, tubular and solid type of human AdCC (**P < 0.01; ***P < 0.001, One-way ANOVA with GraphPad Prism5.0); E. Quantitative of HES1 expression indifferent pathology types of AdCC, increase expression of HES1 were observed from cribriform to tubular or solid types (*P < 0.05; ***P < 0.001, One-way ANOVA with GraphPad Prism5.0).

used for detection and DAPI for nucleus counterstaining. Then the coverlips were mounted on microscope slides with antifade mounting media (Molecular Probes, Carlsbad, CA, USA) and photographed with a fluorescence microscope (Leica).

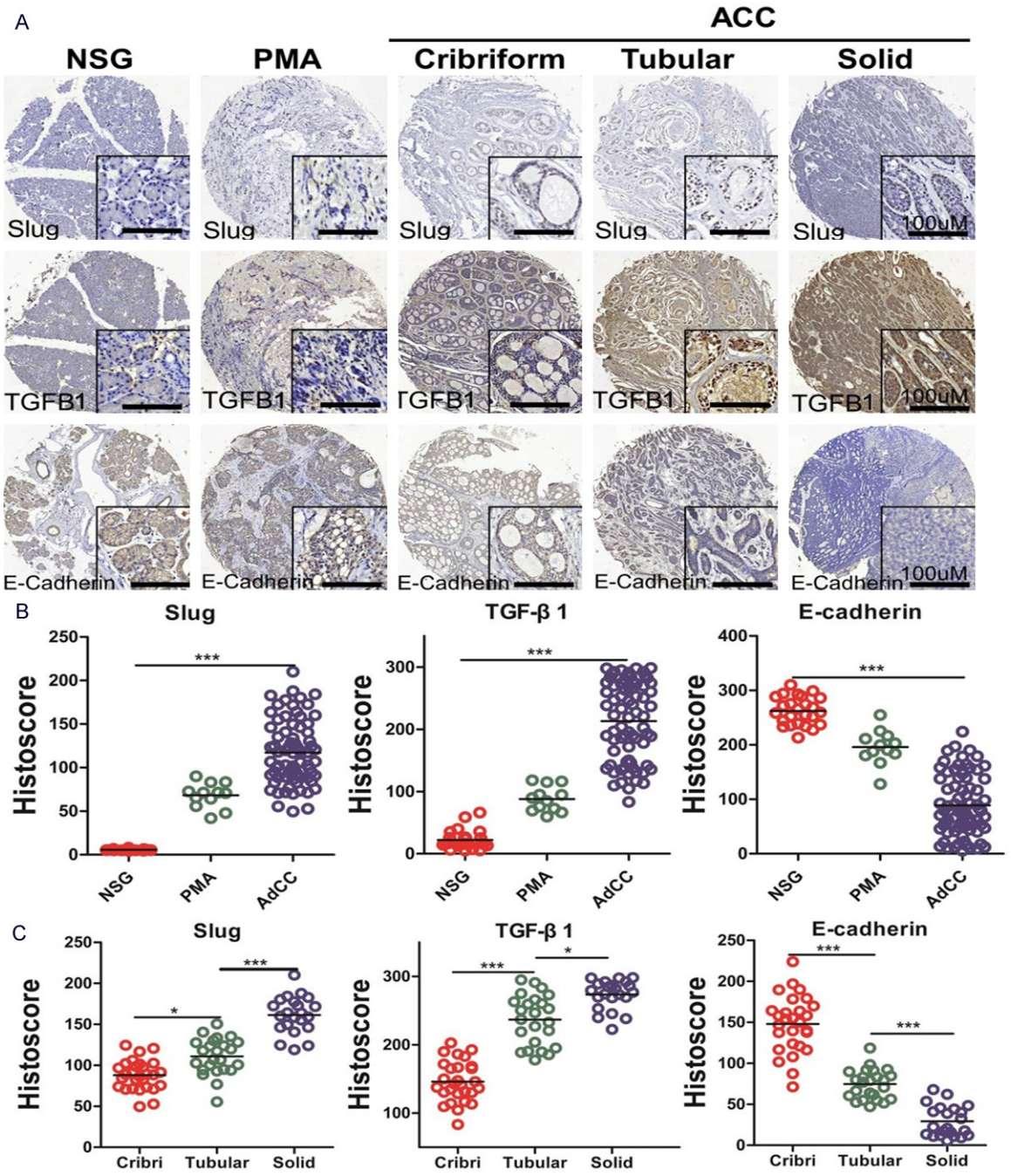

Figure 2. EMT program plays an important role in the AdCC development: A. Representative immunohistochemical staining of Slug, TGF-β1, and E-cadherin in human AdCC tissue (right panel) compared with normal salivary gland (NSG, left panel), pleomorphic adenoma (PMA, middle panel) (Scale bars = 100 μm); B. Quantification of Slug and TGF-β1 expression in NSG, PMA and AdCC, TGF-β1 and Slug were significantly higher when compared with NSG and PMA, while E-cadherin decreased in AdCC when compared with NSG and PMA (***P < 0.001; One-way ANOVA with post-Dunett analysis was used by GraphPad Prism5.0); C. Comparison between different pathology types of Slug and TGF-β1, expression of Slug and TGF-β1 were statistically higher from cribriform to tubular and solid patterns (*P < 0.05; ***P < 0.001, One-way ANOVA with GraphPad Prism5.0).

Wound healing assay

SACC-83 or SACC-LM cells were seeded in 6-well plates (Corning Life Sciences, USA) at 1.0×10^5 cells/well. When cells reached 80% confluence, the center of each well was scratched with a sterile pipette tip to generate a constant gap, and then the cells were contin-

ued incubated with medium containing no FBS to 18 hours. After fixation cells were photographed under phase microscopy and counted as previously described [22].

Transwell invasion assays

In vitro invasion assay was performed using Costar Transwell inserts (#3422, pore size, 8 μm) (Corning, Albany, NY) as described previously [22]. SACC-83 or SACC-LM cells were seeded into the upper chamber coated with Matrigel (BD Biosciences) at a density of 10^4/well in 100 ul serum-free medium, while 10% FBS medium was added to the bottom chamber to stimulate invasion. After incubation for 24 h at 37°C, the cells in the upper chamber were carefully removed with cotton swab and the cells that had invaded through Matrigel were stained with Hematoxylin, and then photographed and quantified. Each assay was conducted in triplicate.

Statistical analysis

Statistical data analysis was performed with GraphPad Prism 5.01 (GraphPad Software, Inc., La Jolla, CA) statistical packages. The Mann–Whitney U test and student t test was used to evaluate differences in the RT-PCR, Western blotting ad immunofluorescence analysis. The One-way ANOVA followed by the post-Turkey or Bonferroni multiple comparison tests was used to analyze the differences in immunohisostaining. Two-tailed Pearson correlation was used for correlated expression of these markers after confirmation of the sample with a Gaussian distribution. $P < 0.05$ was considered statistically significant.

Results

Notch signaling is up-regulated in the AdCC and may be involved in tumor progression

To assess the association of Notch signaling pathway with AdCC progression, we constructed tissue microarray including human AdCC (n = 72), NSG (n = 25) and PMA (n = 12) and incubated the slices with antibodies against NICD (Notch intracellular domain, NICD) and HES1. We observed that NICD expression was almost negative in the normal salivary gland, while increased in PMA and was highest in AdCC. As an effective intracellular component, NICD was mainly found located in the nucleus and cytoplasm at the glandular structure of neoplasm tissues (**Figure 1A**, top panel). We then examined HES1 levels and found fairly weak expression in normal and PMA tissues, whereas AdCC showed strong protein expression in the nucleus (**Figure 1A**, bottom panel). To more precisely and clearly present the differences, we quantified the expression using Aperio ImageScope v12.0 software packages. The results showed that NICD increased consecutively from NSG to PMA and AdCC with statistical significance ($p < 0.05$ and $p < 0.001$, respectively) (**Figure 1B**). Meanwhile, HES1 expression was found significant between AdCC and NSG or PMA tissue ($p < 0.05$) (**Figure 1C**). To further investigate the possible correspondence between Notch signaling and the AdCC progression, we compared the NICD expression in different AdCC subtypes. We showed that NICD increased in a solid pattern than tubular pattern (**Figure 1D**), similar results were observed in HES1 expression (**Figure 1E**). These results suggested Notch signaling increase gradually from the cribriform to solid subtypes of AdCC. These results suggest Notch signaling is up-regulated in the AdCC and may be involved in tumor progression.

EMT program plays an important role in the AdCC development

Epithelial-mesenchymal transition has been proposed to contribute to the invasion and metastasis of AdCC, and we used immunohistochemistry to detect the expression the EMT epithelial marker E-cadherin and EMT inducer TGF-β1 and important transcriptional factor Slug. In our study, EMT transcriptional factor Slug was found enhanced in AdCC when compared with NSG or PMA (**Figure 2A**, top panel). Our results also showed that TGF-β1 was slightly elevated in PMA compared with NSG, while obviously increased in AdCC (**Figure 2A**, middle panel). Meanwhile, we observed the decrease of epithelial marker E-cadherin in AdCC compared with NSG or PMA (**Figure 2A**, bottom panel), indicating the involvement of the EMT process in AdCC development. When we focused on the Slug expression of different pathological subtypes, we found the Slug levels were increased from cribriform to NSG and PMA (**Figure 2C**, left). Then we examined the expression of TGF-β1 and observed that TGF-

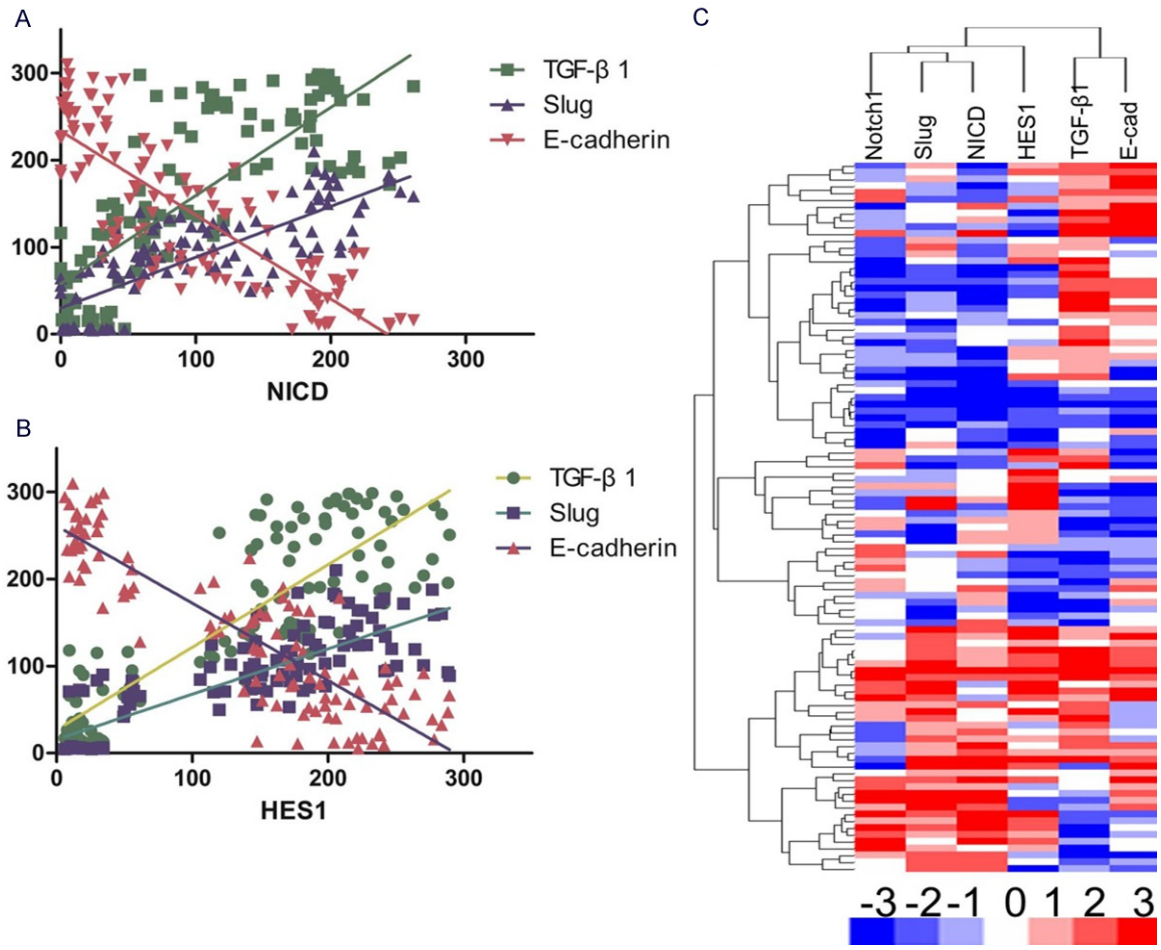

Figure 3. Notch signaling pathway correlate with EMT program: A. The expression of NICD had significant correlations with TGF-β1 ($P < 0.01$, $R = 0.789$), Slug ($P < 0.01$, $R = 0.799$), and E-cadherin ($P < 0.01$, $R = -0.828$) by using the Pearson correlation coefficient test in human tissue microarray; B. The expression of HES1 was closely correlated with TGF-β1 ($P < 0.01$, $R = 0.856$), Slug ($P < 0.01$, $R = 827$) and E-cadherin ($P < 0.01$, $R = -0.884$) in tissue array; C. Hierarchical Clustering of Notch1, NICD, HES1 with TGF-β1, Slug and E-cadherin in human tissue microarray. Histoscores based on quantification using Aperio quantification software and statistics with Graph Pad Prism5.0 Mean ± SEM; 2-tailed Pearson correlation statistics.

β1 were increased in solid subtype of AdCC compared with tubular and cribriform patterns (**Figure 2C**, middle), meanwhile E-cadherin was decreased from cribriform to tubular and cribriform subtypes (**Figure 2C**, right). These facts reflected the gradual loss of epithelial characteristics, but an increase of mesenchymal traits from cribriform to solid subtypes of AdCC. Together, these data indicate that the EMT program plays an important role in the AdCC development.

Notch signaling pathway correlates with EMT program

To determine the correlation of Notch signaling and EMT programs, we carried out correlation analysis and hierarchical clustering. The Spearman rank correlation coefficient was employed to evaluate the relationship between Notch signaling and the EMT program, whereas linear regression analysis for their tendency detection. We found that NICD was statistically associated with TGF-β1 ($P < 0.01$, $R = 0.789$), Slug ($P < 0.01$, $R = 0.799$), and E-cadherin ($P < 0.01$, $R = -0.828$), meanwhile linear regression indicated the positive trendline between NICD with Slug and E-cadherin (**Figure 3A**). Besides, the downstream target of Notch signaling HES1 was observed correlated with TGF-β1 ($P < 0.01$, $R = 0.856$), Slug ($P < 0.01$, $R = 827$) and E-cadherin ($P < 0.01$, $R = -0.884$), also HES1 was found increased in proportion to TGF-β1 while opposite to E-cadherin (**Figure 3B**). To fur-

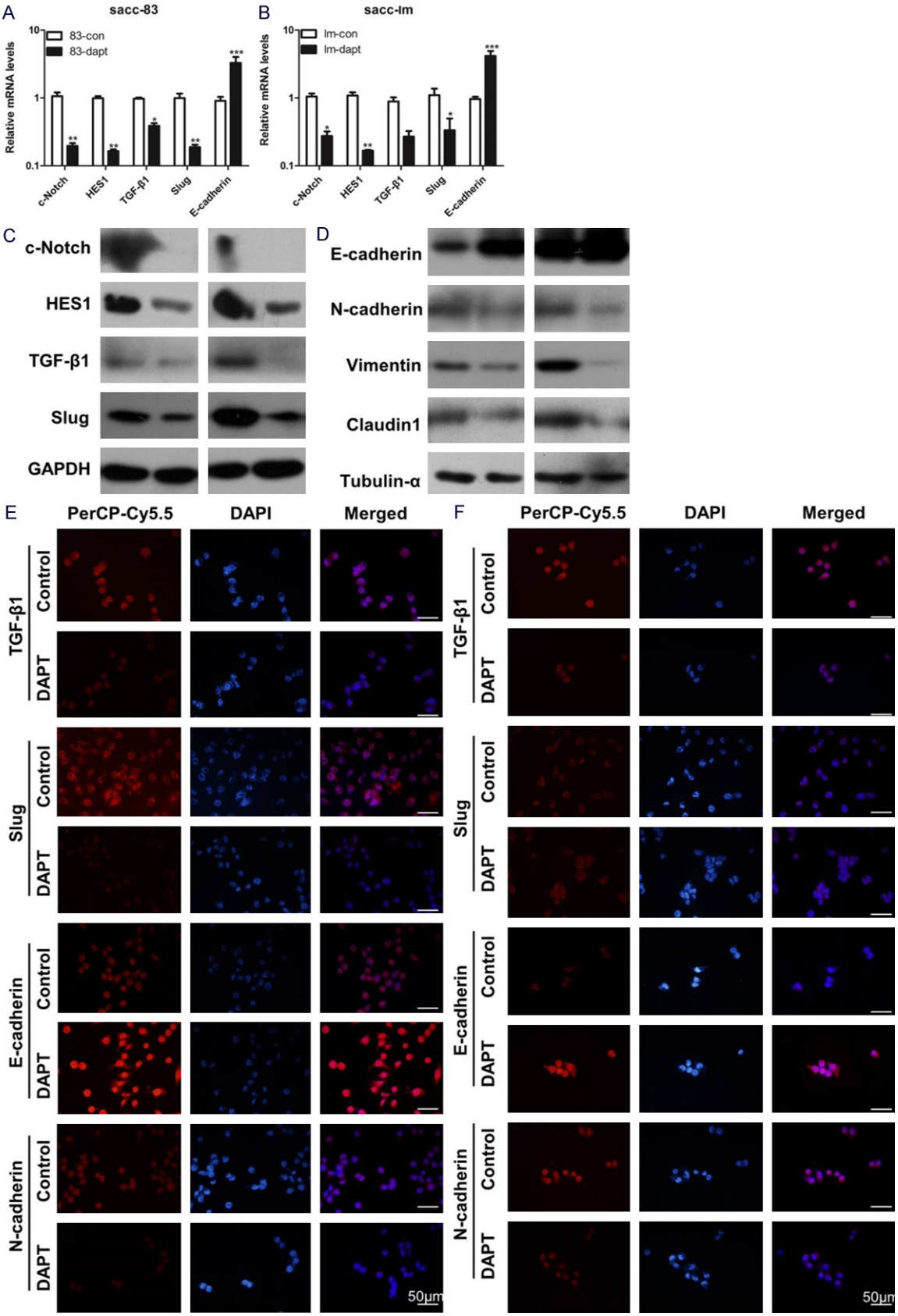

Figure 4. Inhibition of Notch signaling with γ-secretase DAPT decrease epithelial-mesenchymal transitions: A and B. Real-time quantitative PCR shows DAPT inhibition decrease Notch signaling and EMT related proteins in SACC-

83 and SACC-LM cell lines; C and D. Western blotting shows DAPT decrease epithelial-mesenchymal transitions manifesting with decreased regulation factor TGF-β1, slug and mesenchymal markers Vimentin, N-cadherin, also increased epithelial markers E-cadherin and claudin1; E and F. Representative immunofluorescence shows after DAPT treatment, TGF-β1, slug and mesenchymal marker N-cadherin was decreased while epithelial marker E-cadherin increase, bar = 50 μm.

ther probe the interaction between Notch signaling and EMT related proteins, we exerted hierarchical cluster analysis. The results showed close similarity and intimacy between NICD with slug, TGF-β1 with E-cadherin, also we found Notch signaling may confer to EMT program through in combination with TGF-β1 (**Figure 3C**). Together, these results show the correlation of Notch signaling and the EMT program, and Notch signaling may contribute to the invasion and metastasis of AdCC in company with EMT program.

Inhibition of Notch signaling with γ-secretase DAPT decrease EMT progression

To further confirm their relation of Notch signaling and EMT progression, we employed γ-secretase DAPT to block the Notch signaling and detect the change of the EMT program *in vitro* study. SACC-83 which represent a lower invasion and metastasis trend and SACC-LM that show higher invasion and metastasis ability cell lines were employed in our study [23]. We first assessed the mRNA level using real-time RT-PCR and found a clear decrease in the Notch signaling pathway with DAPT inhibition, meanwhile EMT transcriptional factor Slug and inducer TGF-β1 were reduced and E-cadherin was elevated both in SACC-83 and SACC-LM (**Figure 4A**, **4B**; Supplementary Figure 1). We then examined the protein change with Western blotting. In accordance with the mRNA, TGF-β1, slug and mesenchymal markers N-cadherin, Vimentin were decreased while epithelial markers E-cadherin and Claudin1 were increased in SACC-83 and SACC-LM cell lines (**Figure 4C**, **4D**; Supplementary Figure 1). Furthermore, we detect the *in situ* expression of the cell lines with immunofluorescence. Similar results were observed in SACC-83 and SACC-LM cell lines that TGF-β1, slug and N-cadherin were decreased while E-cadherin increased after DAPT blockage (**Figure 4E**, **4F**). These findings suggest Notch signaling may involve in EMT progression to promote invasion and metastasis of AdCC and targeting Notch signaling might be an effective potential therapeutic strategy.

Notch signaling inhibition with DAPT decrease AdCC migration and invasion

Our previous study proved that EMT promote the migration potential of AdCC [15], to determine whether Notch blockade decrease the malignancy of AdCC, wound healing and Boyden chamber invasion assay were carried out to detect the migration and invasion potential. As showed in **Figure 5A** and **5B**, DAPT inhibition dramatically decreased the migration behavior and the cell number of migration was clearly different between control and DAPT treatment group ($p < 0.001$) (**Figure 5C**, **5D**). We then examined the invasion ability change after DAPT inhibition with the Boyden chamber assay. The results showed DAPT treatment notably decreased the invasion cells compared with the control group in SACC-LM, similar results were observed in SACC-83 with a different degree (**Figure 5E**, **5F**). These data clearly indicate Notch promote EMT-induced migration and invasion and may be a novel therapeutic target.

Discussion

Accumulating evidence has suggested that EMT plays an important roles in the invasion and metastasis of carcinoma development [11]. Bedsides, Notch signaling have been implicated as important molecular events in recent next generation sequencing studies of AdCC, but the specific mechanism is still unclear and their relation with EMT remained to study. Thus, we are wondering whether Notch signaling and EMT are hidden behind the invasion and metastasis of AdCC. In this study, we utilized custom-made tissue microarray to evaluate the expression of Notch signaling I AdCC and γ-secretase inhibitor DAPT to investigate the role of Notching signaling and EMT, we found Notch signaling promote invasion and metastasis of AdCC conspired with the EMT program. Thus, targeting Notch signaling may provide novel insights into the mechanism of invasion and metastasis of AdCC as well as possible therapeutic interventions.

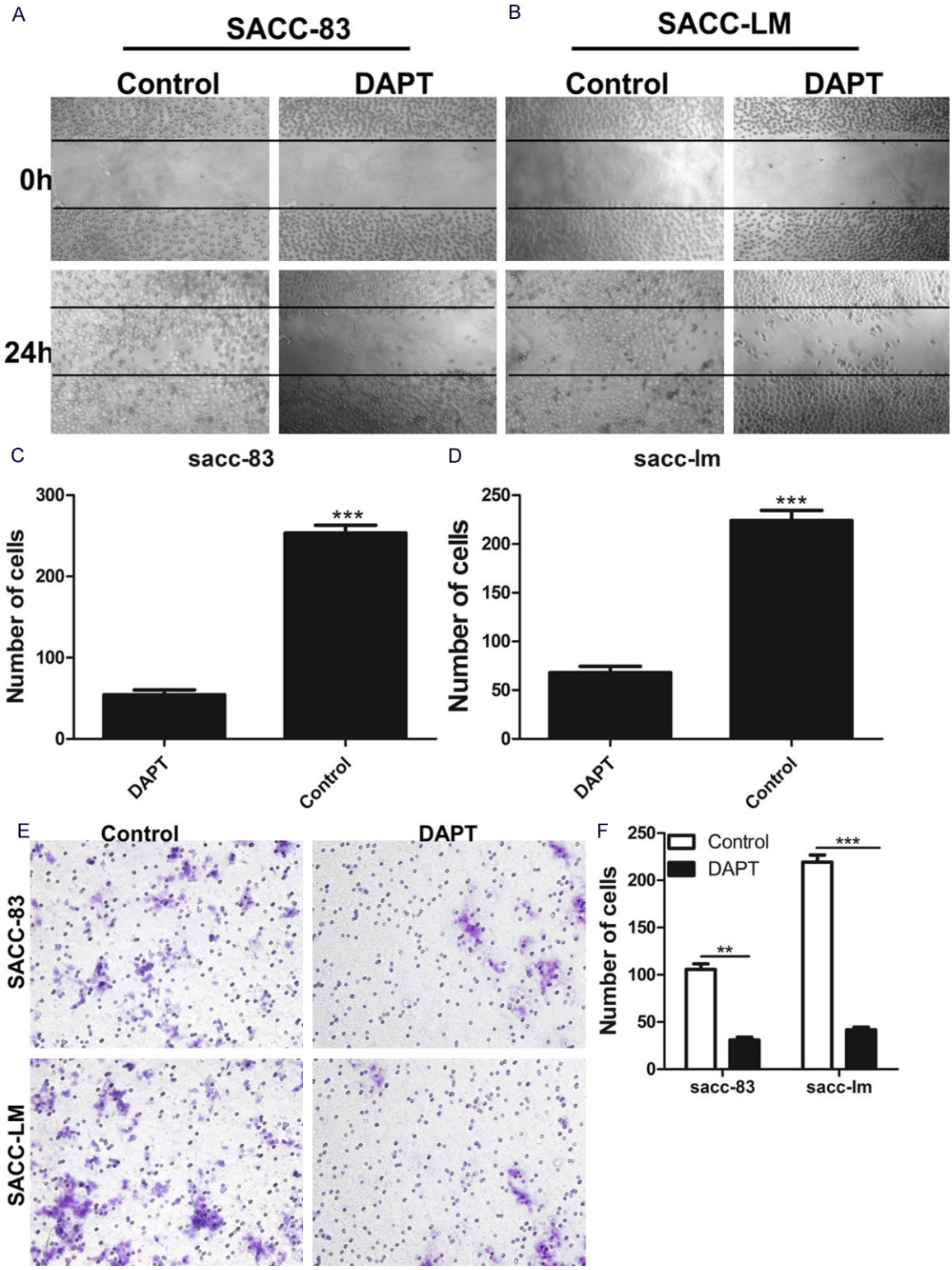

Figure 5. Notch signaling inhibition decrease AdCC cell lines migration and invasion. A and B. Scratch assay shows treatment with DAPT 10 mmol/L 24 hours significantly decrease the mobility of SACC-83 and SACC-LM cell line; C and D. quantification of cell numbers with ImageJ "cell counter" module indicate the statistical significance of the difference (Mean ± SD; ***P < 0.001, student *t*-test with GraphPad Prism5.0); E. Transwell assay shows the migration ability of sac-83 and SACC-LM were impaired when treated with DAPT compared with control group; F. Quantification of cell numbers with ImageJ "cell counter" module (Mean ± SD; ***P < 0.001, student *t*-test with GraphPad Prism5.0).

Notch signaling has emerged as a potent regulatory mechanism for the regulation of EMT progression. In lung cancer, Notch1 was found increased in chemotherapy resistant patients and inhibition of Notch1 can reverse the EMT phenotype thereby potentially increasing drug sensitivity of lung cancer cells [23]. Meanwhile, over-expression of NICD in immortalized endothelial cells induces EMT accompanied by oncogenictransformation,withcorrespondinginduction of snail and repression of VE-cadherin expression [24]. Also, the next generation sequencing (NGS) reveals that about 13% NOTCH1 gene mutations and exon sequencing in a series of 24 ACC samples get similar conclusions [7, 8]. Our results showed that NICD and its target gene HES1 were increased from NSG to PMA and AdCC. Bell et al [25] also observed elevated expression levels of Notch signaling proteins in AdCC tissue relative to normal salivary gland tissues. These data show Notch signaling is associated with human AdCC progression while the mechanism is still not clear.

The EMT program is initiated by signaling pathways that respond to extracellular cues, among which transforming growth factor-β family signaling (especially TGF-β1) has a predominant role that mediates the EMT process. In breast cancer, dysregulated TGF-β1 was observed to up-regulate long noncoding RNAs (lncRNA) to promote metastasis and associated with poor prognosis [26]. For hepatocellular carcinoma, TGF-β1 combined with CXCR4 promotes EMT and contributes to tumor progression and dissemination [27]. In this study, we showed increased levels of TGF-β1 from NSG to PMA and AdCC, while significance between AdCC and NSG was observed. Slug, one of the three vertebrate SNAIL proteins, activates the EMT program by binding to E-box DNA sequences through their carboxy-terminal zinc-finger domains. We showed in the study that Slug expression levels in AdCC are remarkably higher than NSG or PMA, which is similar to other reports in the bladder, pancreatic and esophageal cancer [28-30]. TGF-β1 induces EMT by acting at the transcriptional, translational and post-translational levels. Through Smad signaling to activate transcription factors and increase their activity, also TGF-β1-Slug pathway induces PI3K-AKT-mTORC1 to up-regulate mesenchymal components and restrain cell junctions and cytoskeleton stability [31]. To verify the relation of TGF-β1 and Slug, Pearson correlation analysis was conducted, and we found TGF-β1 was related to Slug while negatively correlated with E-cadherin as expected. Besides the increase of EMT inductor TGF-β1 and transcription factor Slug, loss of E-cadherin has been considered a hallmark of the EMT program. The tissue microarray results indicated a decrease of E-cadherin in AdCC compared with NSG or PMA. Thus, these results validate that TGF-β1/Slug induced EMT and program plays an important role in the AdCC development, although further studies are needed to elucidate the exact mechanism.

To investigate the specific mechanism of Notch signaling in AdCC and their relation with EMT, we used γ-secretase inhibitor DAPT to block the Notch signaling pathway. We showed in this work that inhibition of Notch could notably decrease the TGF-β1, Slug and E-cadherin in the process of EMT, both in mRNA and protein levels through real-time RT-PCR and Western blotting. This is consistent with the discovery that inhibition of the Jagged/Notch signaling pathway decreased EMT in human retinal pigment epithelium cells and thus prevent proliferative diabetic retinopathy [32]. Besides, cooperation between different regulation or transcription factors is an important hallmark of EMT induction. Despite the multiple extracellular signal and molecules, TGF-β1 has been considered as an integrator by using Slug (SNAIL family) as its downstream master effectors. It was reported that targeting TGF-β and Wnt7b signaling in pancreatic ductal adenocarcinoma may disrupt epithelial-to-mesenchymal transition and attenuated tumor growth and invasion [33]. We showed in our study that Notch blockade could simultaneously decrease TGF-β1 and Slug, which indicated the possible mechanism for Notch signaling. Furthermore, DAPT inhibition could dramatically decrease the migration and invasion ability induced by EMT program. Together, these functional crosstalks indicate Notch signaling may induce EMT program to promote invasion and metastasis of AdCC and targeting Notch signaling an effective therapeutic choice.

In conclusion, this study has confirmed the important roles of Notch signaling is up-regulated in the AdCC and may be involved in tumor progression. Our work has also revealed that Notch signaling promotes invasion and metastasis of AdCC conspired with EMT program and

blockade of Notch signaling. Thus, targeting Notch signaling may provide new insights into the mechanism of invasion and metastasis of AdCC as well as possible therapeutic interventions.

Acknowledgements

This study was supported by the National Natural Science Foundation of China (81072203, 81272963, 81472528) to Zhi-Jun Sun, (81371106) to Lu Zhang, (81272946, 81472529) to Wen-Feng Zhang, and (81170977) to Yi-Fang Zhao.

Disclosure of conflict of interest

None.

Address correspondence to: Zhi-Jun Sun or Wen-Feng Zhang, Department of Oral Maxillofacial-Head Neck Oncology, School and Hospital of Stomatology, Wuhan University, Wuhan, 430079, China. E-mail: zhijundejia@163.com (ZJS), zhangwf59@163.com (WFZ)

References

[1] Sung MW, Kim KH, Kim JW, Min YG, Seong WJ, Roh JL, Lee SJ, Kwon TK and Park SW. Clinicopathologic predictors and impact of distant metastasis from adenoid cystic carcinoma of the head and neck. Arch Otolaryngol Head Neck Surg 2003; 129: 1193-1197.

[2] Fordice J, Kershaw C, El-Naggar A and Goepfert H. Adenoid cystic carcinoma of the head and neck: predictors of morbidity and mortality. Arch Otolaryngol Head Neck Surg 1999; 125: 149-152.

[3] Artavanis-Tsakonas S, Rand MD and Lake RJ. Notch signaling: cell fate control and signal integration in development. Science 1999; 284: 770-776.

[4] Miyamoto S and Rosenberg DW. Role of Notch signaling in colon homeostasis and carcinogenesis. Cancer Sci 2011; 102: 1938-1942.

[5] Lonardo E, Hermann PC, Mueller MT, Huber S, Balic A, Miranda-Lorenzo I, Zagorac S, Alcala S, Rodriguez-Arabaolaza I, Ramirez JC, Torres-Ruiz R, Garcia E, Hidalgo M, Cebrian DA, Heuchel R, Lohr M, Berger F, Bartenstein P, Aicher A and Heeschen C. Nodal/Activin signaling drives self-renewal and tumorigenicity of pancreatic cancer stem cells and provides a target for combined drug therapy. Cell Stem Cell 2011; 9: 433-446.

[6] Stransky N, Egloff AM, Tward AD, Kostic AD, Cibulskis K, Sivachenko A, Kryukov GV, Lawrence MS, Sougnez C, McKenna A, Shefler E, Ramos AH, Stojanov P, Carter SL, Voet D, Cortes ML, Auclair D, Berger MF, Saksena G, Guiducci C, Onofrio RC, Parkin M, Romkes M, Weissfeld JL, Seethala RR, Wang L, Rangel-Escareno C, Fernandez-Lopez JC, Hidalgo-Miranda A, Melendez-Zajgla J, Winckler W, Ardlie K, Gabriel SB, Meyerson M, Lander ES, Getz G, Golub TR, Garraway LA and Grandis JR. The mutational landscape of head and neck squamous cell carcinoma. Science 2011; 333: 1157-1160.

[7] Ho AS, Kannan K, Roy DM, Morris LG, Ganly I, Katabi N, Ramaswami D, Walsh LA, Eng S, Huse JT, Zhang J, Dolgalev I, Huberman K, Heguy A, Viale A, Drobnjak M, Leversha MA, Rice CE, Singh B, Iyer NG, Leemans CR, Bloemena E, Ferris RL, Seethala RR, Gross BE, Liang Y, Sinha R, Peng L, Raphael BJ, Turcan S, Gong Y, Schultz N, Kim S, Chiosea S, Shah JP, Sander C, Lee W and Chan TA. The mutational landscape of adenoid cystic carcinoma. Nat Genet 2013; 45: 791-798.

[8] Stephens PJ, Davies HR, Mitani Y, Van Loo P, Shlien A, Tarpey PS, Papaemmanuil E, Cheverton A, Bignell GR, Butler AP, Gamble J, Gamble S, Hardy C, Hinton J, Jia M, Jayakumar A, Jones D, Latimer C, McLaren S, McBride DJ, Menzies A, Mudie L, Maddison M, Raine K, Nik-Zainal S, O'Meara S, Teague JW, Varela I, Wedge DC, Whitmore I, Lippman SM, McDermott U, Stratton MR, Campbell PJ, El-Naggar AK and Futreal PA. Whole exome sequencing of adenoid cystic carcinoma. J Clin Invest 2013; 123: 2965-2968.

[9] Thiery JP. Epithelial-mesenchymal transitions in tumour progression. Nat Rev Cancer 2002; 2: 442-454.

[10] Lee MY and Shen MR. Epithelial-mesenchymal transition in cervical carcinoma. Am J Transl Res 2012; 4: 1-13.

[11] Thiery JP, Acloque H, Huang RY and Nieto MA. Epithelial-mesenchymal transitions in development and disease. Cell 2009; 139: 871-890.

[12] Listinsky JJ, Siegal GP and Listinsky CM. The emerging importance of alpha-L-fucose in human breast cancer: a review. Am J Transl Res 2011; 3: 292-322.

[13] Labelle M, Begum S and Hynes RO. Direct signaling between platelets and cancer cells induces an epithelial-mesenchymal-like transition and promotes metastasis. Cancer Cell 2011; 20: 576-590.

[14] Sethi S, Macoska J, Chen W and Sarkar FH. Molecular signature of epithelial-mesenchymal transition (EMT) in human prostate cancer bone metastasis. Am J Transl Res 2010; 3: 90-99.

[15] Jia J, Zhang W, Liu JY, Chen G, Liu H, Zhong HY, Liu B, Cai Y, Zhang JL and Zhao YF. Epithelial

mesenchymal transition is required for acquisition of anoikis resistance and metastatic potential in adenoid cystic carcinoma. PLoS One 2012; 7: e51549.
[16] Barnes L. Pathology & genetics: head and neck tumours. World Health Organization, 2005.
[17] Huang CF, Zhang L, Ma SR, Zhao ZL, Wang WM, He KF, Zhao YF, Zhang WF, Liu B and Sun ZJ. Clinical significance of Keap1 and Nrf2 in oral squamous cell carcinoma. PLoS One 2013; 8: e83479.
[18] Wang YF, Zhang W, He KF, Liu B, Zhang L, Zhang WF, Kulkarni AB, Zhao YF and Sun ZJ. Induction of autophagy-dependent cell death by the survivin suppressant YM155 in salivary adenoid cystic carcinoma. Apoptosis 2014; 19: 748-758.
[19] Sun ZJ, Zhang L, Hall B, Bian Y, Gutkind JS and Kulkarni AB. Chemopreventive and Chemotherapeutic Actions of mTOR Inhibitor in Genetically Defined Head and Neck Squamous Cell Carcinoma Mouse Model. Clin Cancer Res 2012; 18: 5304-5313.
[20] Eisen MB, Spellman PT, Brown PO and Botstein D. Cluster analysis and display of genome-wide expression patterns. Proc Natl Acad Sci U S A 1998; 95: 14863-14868.
[21] Saldanha AJ. Java Treeview--extensible visualization of microarray data. Bioinformatics 2004; 20: 3246-3248.
[22] Zhang L, Sun ZJ, Bian Y and Kulkarni AB. MicroRNA-135b acts as a tumor promoter by targeting the hypoxia-inducible factor pathway in genetically defined mouse model of head and neck squamous cell carcinoma. Cancer Lett 2013; 331: 230-238.
[23] Wang L, Wang Y, Bian H, Pu Y and Guo C. Molecular characteristics of homologous salivary adenoid cystic carcinoma cell lines with different lung metastasis ability. Oncol Rep 2013; 30: 207-212.
[24] Timmerman LA, Grego-Bessa J, Raya A, Bertran E, Perez-Pomares JM, Diez J, Aranda S, Palomo S, McCormick F, Izpisua-Belmonte JC and de la Pompa JL. Notch promotes epithelial-mesenchymal transition during cardiac development and oncogenic transformation. Genes Dev 2004; 18: 99-115.
[25] Bell D, Hanna EY, Miele L, Roberts D, Weber RS and El-Naggar AK. Expression and significance of notch signaling pathway in salivary adenoid cystic carcinoma. Ann Diagn Pathol 2014; 18: 10-13.
[26] Gregory PA, Bert AG, Paterson EL, Barry SC, Tsykin A, Farshid G, Vadas MA, Khew-Goodall Y and Goodall GJ. The miR-200 family and miR-205 regulate epithelial to mesenchymal transition by targeting ZEB1 and SIP1. Nat Cell Biol 2008; 10: 593-601.
[27] Yuan JH, Yang F, Wang F, Ma JZ, Guo YJ, Tao QF, Liu F, Pan W, Wang TT, Zhou CC, Wang SB, Wang YZ, Yang Y, Yang N, Zhou WP, Yang GS and Sun SH. A Long Noncoding RNA Activated by TGF-beta Promotes the Invasion-Metastasis Cascade in Hepatocellular Carcinoma. Cancer Cell 2014; 25: 666-681.
[28] Jing Y, Cui D, Guo W, Jiang J, Jiang B, Lu Y, Zhao W, Wang X, Jiang Q, Han B and Xia S. Activated androgen receptor promotes bladder cancer metastasis via Slug mediated epithelial-mesenchymal transition. Cancer Lett 2014; 348: 135-145.
[29] Li A, Morton JP, Ma Y, Karim SA, Zhou Y, Faller WJ, Woodham EF, Morris HT, Stevenson RP, Juin A, Jamieson NB, MacKay CJ, Carter CR, Leung HY, Yamashiro S, Blyth K, Sansom OJ and Machesky LM. Fascin is regulated by slug, promotes progression of pancreatic cancer in mice, and is associated with patient outcomes. Gastroenterology 2014; 146: 1386-1396.
[30] Hasan MR, Sharma R, Saraya A, Chattopadhyay TK, DattaGupta S, Walfish PG, Chauhan SS and Ralhan R. Slug is a predictor of poor prognosis in esophageal squamous cell carcinoma patients. PLoS One 2013; 8: e82846.
[31] Yang J and Weinberg RA. Epithelial-mesenchymal transition: at the crossroads of development and tumor metastasis. Contrib Sens Physiol 2008; 14: 818-829.
[32] Chen X, Xiao W, Liu X, Zeng M, Luo L, Wu M, Ye S and Liu Y. Blockade of Jagged/Notch pathway abrogates transforming growth factor beta2-induced epithelial-mesenchymal transition in human retinal pigment epithelium cells. Curr Mol Med 2014; 14: 523-534.
[33] Gore AJ, Deitz SL, Palam LR, Craven KE and Korc M. Pancreatic cancer-associated retinoblastoma 1 dysfunction enables TGF-beta to promote proliferation. J Clin Invest 2014; 124: 338-352.

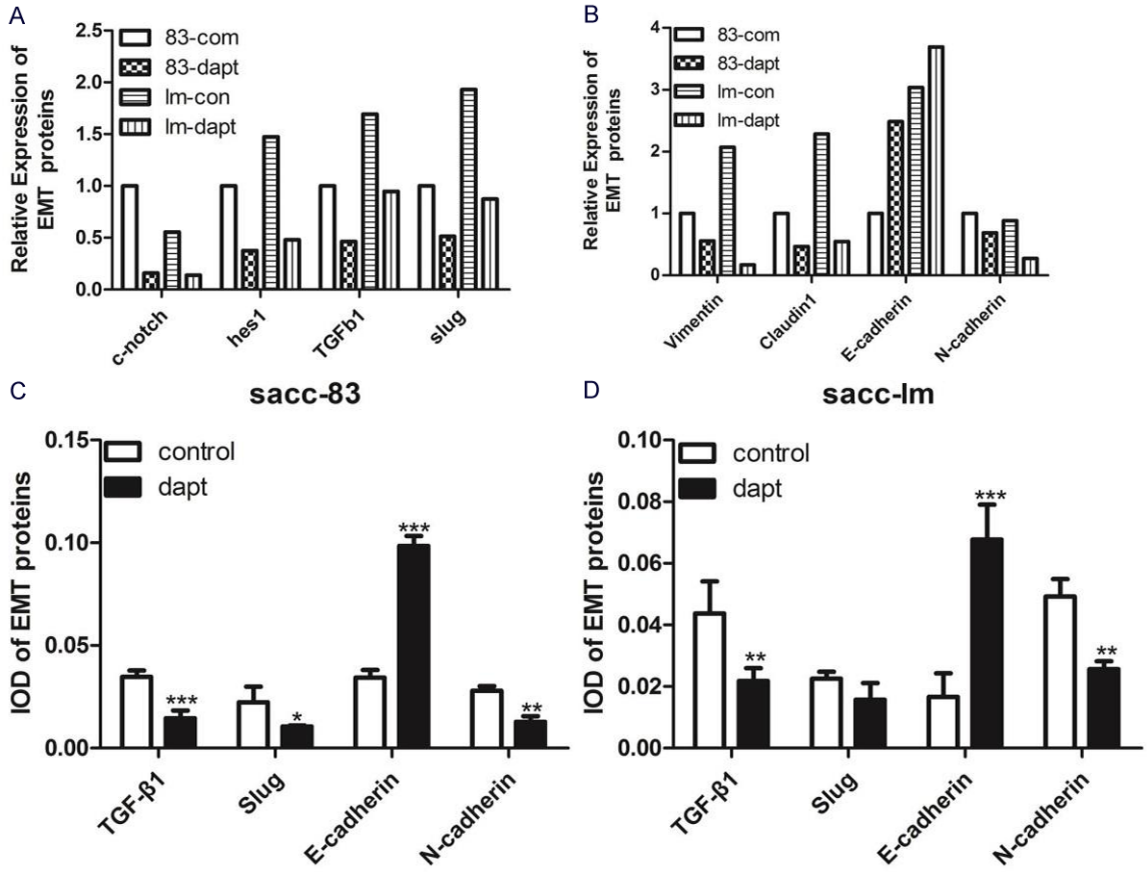

Supplementary Figure 1. Inhibition of Notch signaling with γ-secretase DAPT decrease epithelial-mesenchymal transitions. A and B. Quantification of western blotting results withImage J gel analysis, SACC-83 untreatedgroup was used as control; C and D. Quantification of immunofluorescence with NIH ImageJ 1.46r (Mean ± SD; *P < 0.05; **P < 0.01; ***P < 0.001, One-way ANOVA with GraphPad Prism5.0).

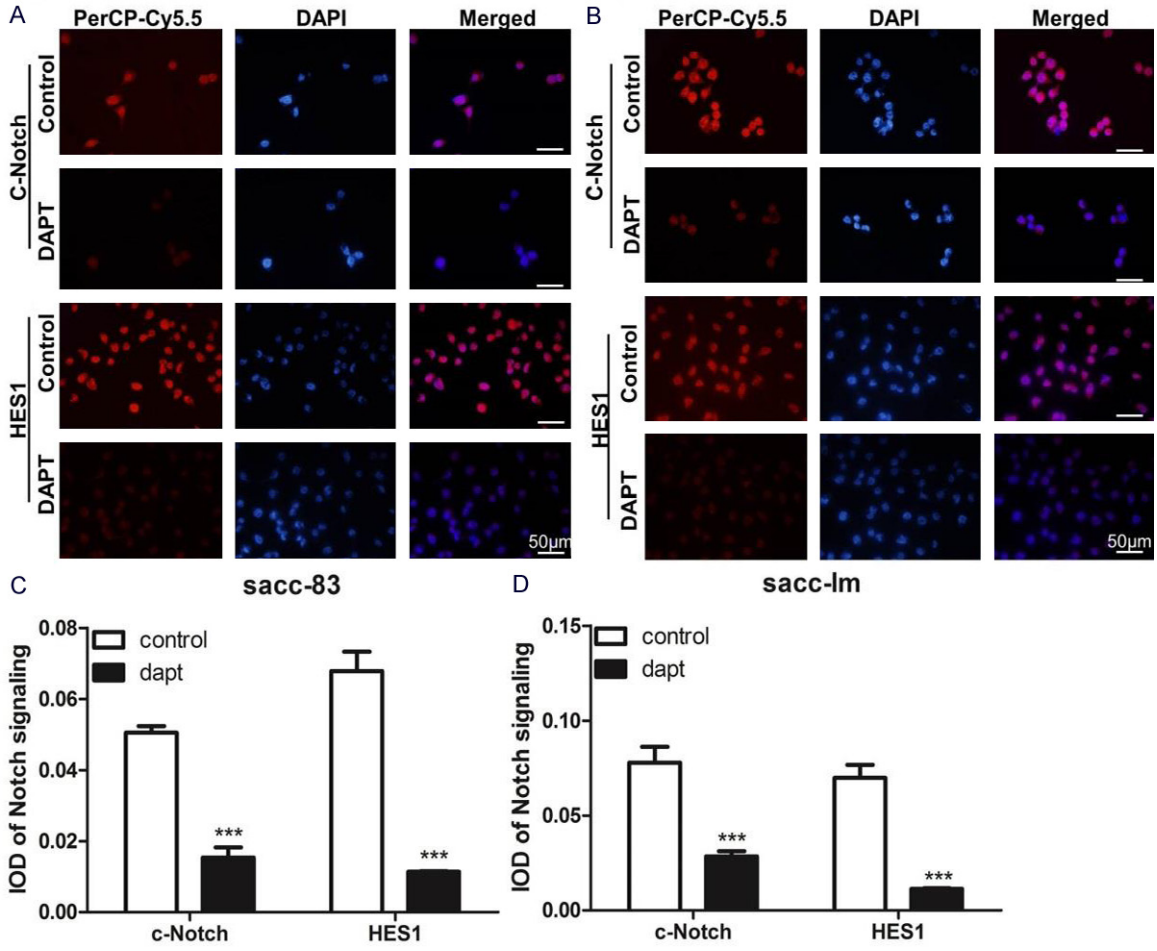

Supplementary Figure 2. DAPT treatment inhibits the Notch signaling pathway. A. Immunofluroscence shows treatment with DAPT 10 mmol/L 24 hours decrease the expression of Cleaved-Notch, and HES1 in SACC-83 and SACC-LM cell lines; B. Quantification of immunofluorescence for SACC-83 andSACC-LM with ImageJ, IOD for mean integrated optical density and calculated with total optical density divided by the area.